



Article

# The Effect of Mineral Fillers on the Rheological and Performance Properties of Self-Compacting Concretes in the Production of Reinforced Concrete Products

Meiram M. Begentayev<sup>1</sup>, Erzhan I. Kuldeyev<sup>1</sup>, Daniyar A. Akhmetov<sup>1</sup>, Zhanar O. Zhumadilova<sup>1,\*</sup> ,  
Dossym K. Suleyev<sup>1</sup>, Yelbek B. Utepov<sup>2</sup> , Talal Awwad<sup>3,\*</sup> and Mussa T. Kuttybay<sup>4</sup>

<sup>1</sup> Satbayev University, Almaty 050000, Kazakhstan; m.begentayev@satbayev.university (M.M.B.); kuldeyev@satbayev.university (E.I.K.); d.a.akhmetov@satbayev.university (D.A.A.); suleyevd@gmail.com (D.K.S.)

<sup>2</sup> Department of Civil Engineering, L.N. Gumilyov Eurasian National University, Astana 010000, Kazakhstan; utepov\_yeb@enu.kz

<sup>3</sup> Soils and Foundations Department, Emperor Alexander I St. Petersburg State Transport University, Saint Petersburg 190031, Russia

<sup>4</sup> Department of Building materials and expertise in construction, Auezov University, Shymkent 160012, Kazakhstan; m\_kuttybay@mail.ru

\* Correspondence: z.zhumadilova@satbayev.university (Z.O.Z.); awwad@pgups.ru (T.A.)

**Abstract:** This study investigates the impact of widely used mineral fillers in self-compacting concrete compositions applied in vibration-free reinforced concrete production technology, as a means of enhancing rheological characteristics and cost-effectiveness. Three distinct types of mineral fillers, including the well-studied fillers microsilica and metakaolin, as well as the lesser-explored filler Kazakhstani natural opal-chalcedony opoka, are examined in this research. In addition to the evaluation of conventional rheological and performance properties of concretes containing these fillers, the internal processes within the cement–filler matrix are analyzed. This includes X-ray phase analysis and microstructural examination of cement hydration products in combination with a superplasticizer and each of the three minerals. The findings confirm the potential for optimizing the rheological parameters of the concrete mixture by substituting up to 15% of the cement with mineral fillers, achieving optimal viscosity and workability. It is established that compositions with the addition of microsilica and metakaolin have a more homogeneous structure, mainly represented by low-basicity calcium hydrosilicates of the CSH(B) type, along with an increase in compressive strength of up to 10%. The addition of these mineral fillers to C30/35 strength class self-compacting concrete resulted in improved frost resistance up to F300, a reduction in volumetric water absorption by up to 30%, and a decrease in shrinkage deformations by 32%. The developed SCC compositions have successfully passed production testing and are recommended for implementation in the operational processes of reinforced concrete product manufacturing plants.

**Keywords:** frost resistance; water absorption; shrinkage deformations; mineral fillers; cement; self-compacting concrete



Academic Editor: Peng Zhang

Received: 15 March 2025

Revised: 29 April 2025

Accepted: 2 May 2025

Published: 6 May 2025

**Citation:** Begentayev, M.M.; Kuldeyev, E.I.; Akhmetov, D.A.; Zhumadilova, Z.O.; Suleyev, D.K.; Utepov, Y.B.; Awwad, T.; Kuttybay, M.T. The Effect of Mineral Fillers on the Rheological and Performance Properties of Self-Compacting Concretes in the Production of Reinforced Concrete Products. *J. Compos. Sci.* **2025**, *9*, 235. <https://doi.org/10.3390/jcs9050235>

**Copyright:** © 2025 by the authors. Licensee MDPI, Basel, Switzerland. This article is an open access article distributed under the terms and conditions of the Creative Commons Attribution (CC BY) license (<https://creativecommons.org/licenses/by/4.0/>).

## 1. Introduction

Self-compacting concrete (SCC) is widely applied in global practice for both cast-in-place and precast technologies in general construction. The use of SCC eliminates the need for vibration and heat treatment during the production of reinforced concrete elements,

contributing to improved homogeneity and durability of concrete. Additionally, SCC reduces labor costs, decreases maintenance expenses for technological equipment, and improves working conditions. The global construction industry faces increasing demands for reduction of the environmental impact of cement production, particularly through the use of industrial by-products. Developing SCC with mineral fillers supports international efforts to lower CO<sub>2</sub> emissions and advance sustainable building practices in line with the UN Sustainable Development Goals (SDGs) [1]. The application of SCC in cast-in-place construction has been extensively studied by researchers from Europe and Asia. Numerous laboratory and industrial tests have been carried out, and operating production lines have been established. In the Republic of Kazakhstan, this field is still under development, mainly at the stage of research and small-scale production at individual plants. Currently, SCC is not widely adopted in the national construction industry. The implementation of SCC technologies in Kazakhstan has faced several limiting factors. These include a lack of financial support for research in this field, the absence of national standards for this type of concrete (with existing regulations covering only test methods), and weak cooperation between science and industry. Although interest in SCC has grown in recent years, research on the production of SCC using local raw materials remains limited [2]. Despite these challenges, some manufacturing companies in Kazakhstan see SCC technology as a promising way to achieve significant economic benefits. These include eliminating vibration during production, reducing binder consumption, improving the homogeneity and durability of concrete, lowering labor costs, minimizing equipment maintenance expenses, and improving working conditions. It has been established that the use of mineral fillers as independent components in concrete mixtures is an effective method for improving the economic efficiency of SCC, by reducing both the cost per cubic meter and cement consumption, while enhancing the construction and technological properties of the material [3]. Mineral fillers are widely used in international practice, particularly in high-performance concretes, including SCC. Moreover, the use of natural and industrial fine mineral fillers in SCC reduces the cement content, thereby minimizing the environmental impact of concrete production [4,5]. In addition, the incorporation of mineral fillers into SCC significantly affects its rheological properties [6]. However, the use of these fillers requires caution, as improving one property may worsen another. Therefore, the study of the rheological properties of SCC containing mineral fillers requires a comprehensive approach that considers all key rheological parameters, including flowability and viscosity, to accurately assess its potential applications [7]. Despite numerous studies on SCC incorporating mineral fillers, there is a lack of comprehensive data regarding the optimal replacement levels of silica fume and fly ash that ensure a balance between rheological performance, mechanical properties, and sustainability, particularly when using region-specific raw materials. A review of global research shows that data on the use of mineral fillers in SCC are often contradictory. There is insufficient information on the optimal filler content in the cement matrix, the structure of hardened cement paste with various mineral fillers, and the activity of fillers in the “cement–water” system [8]. Silica fume, as a fine mineral modifier in high-performance concrete, has been well studied [9]. However, several pozzolanic and inert fillers retrieved in Kazakhstan, such as metakaolin, diatomite, and zeolites, remain weakly explored. Furthermore, the properties of these natural raw materials can vary significantly depending on their geological origin [10]. It is known that the activity of metakaolin in the “cement–water” system is determined by its silica and alumina content. The use of metakaolin promotes the early formation of hydration products, which contributes to improved strength development [11]. According to the experimental results presented in [12], the use of metakaolin in SCC results in improved mechanical properties compared to conventional SCC mixtures. The pozzolanic reactivity of natural diatomite

is linked to its metastable state and primarily depends on its chemical and mineralogical composition, with particle fineness having a lesser influence [13]. Despite some application challenges, the use of locally available mineral raw materials is one of the key factors for ensuring the economic efficiency and environmental sustainability of SCC production and use. In this context, the study of various natural and industrial mineral resources that are typical of different regions of Kazakhstan is highly relevant for their application in SCC [14]. In general, the introduction of active mineral fillers into cement systems ensures the required rheological conditions for producing high-performance and workable mixtures, the formation of a dense material structure, and, consequently, increased concrete strength. It is important to note that the hydration and hardening processes of SCC depend on the curing temperature and humidity, the type and chemical composition of the cement, the properties of superplasticizers, and many other factors. From the moment water is added, these factors influence hardening kinetics, colloidal-chemical processes, and the crystallization of hydrates [15]. Furthermore, the inclusion of mineral fillers in SCC affects its rheological behavior.

This study aims to introduce SCC technology into precast concrete production and improve the performance characteristics of reinforced concrete products manufactured with this type of concrete. The objective of the study is the potential use of industrial waste and natural resources of the Republic of Kazakhstan in the production of SCC and products constructed from it. The novelty of this work lies in the systematic evaluation of locally sourced mineral fillers in SCC compositions, providing new insights into the combined effect of silica fume and fly ash on the material's fresh- and hardened-state properties under regional conditions. The purpose of this research is to develop medium-strength SCC mixtures with improved rheological and performance characteristics for technological lines producing high-quality reinforced concrete products.

To achieve this goal, a study was carried out on the influence and combined effects of three widely used mineral modifiers in filled cement systems. The optimal content of mineral components in the concrete mixture was determined, and factors influencing the formation of a densely packed material structure and the enhancement of performance properties were identified. The increase in the density of cement composites at the optimal level of mineral filler content is explained by several factors: the orienting effect of filler particles on cement hydration products and the formation of cluster structures; the use of materials with similar crystallochemical properties; the formation of additional bonds due to chemical interactions when pozzolanic additives are introduced; and the reduction in porosity [16]. The present study's hypotheses were investigated using scanning electron microscopy (SEM) [17] and X-ray diffraction (XRD) [18] methods. The study presents a set of technological solutions for developing high-performance concrete mixtures with specified properties, based on local raw materials intended for the utilization of ferroalloy wastes [19].

## 2. Materials and Methods

The investigation comprised seven sequential stages, each meticulously designed to address distinct objectives:

1. Selecting fundamental materials for the study, in alignment with the normative documents governing these specific materials [20–24].
2. Calculating and selecting the reference composition of mortar samples of SCC [25–27].
3. Inputting the calculated quantity of 3 popular types of mineral fillers, and determining the main rheological parameters [26,28–31].
4. Examining the macrostructure of the acquired samples by visual observation and their microstructure by SEM [17], and conducting XRD [18].

5. Selecting the reference composition of the main class of heavy SCC (with a density of 2200–2500 kg/m<sup>3</sup>) used in the production of C30/35 [32].
6. Determining the rheological characteristics of the SCC [26,30,31].
7. Verifying concrete samples for operational reliability by testing for frost resistance [33] and volumetric water absorption [34], by measuring shrinkage deformations [35] at 28 days of age.

The calculations were made using the method of mixture composition selection, based on the method of Hitoshi Okamura, the founder of SCC and a professor at the University of Tokyo, which was developed to design a mixture with the following parameters [25]: a high content of fine fractions; a coarse aggregate size of 5–20 mm; the use of Portland cement of average performance; and an air content of 4–7%.

### 2.1. Description and Characteristics of Materials Used

Table 1 illustrates the attributes of the binder (cement) from Heidelberg Cement, LLP (Shymkent, Kazakhstan), selected following the specifications outlined in [20].

**Table 1.** Cement characteristics.

Cement Grade	Compressive Strength at 28 Days of Age, at Least, MPa	Start of Setting, Not Earlier Than, min	Bulk Density, kg/m <sup>3</sup>	Quantity per 1 m <sup>3</sup> of Heavy SCC, kg
CEM I 42.5 R *	47.2	124	1250	400–550

\* In [20], the interpretation of CEM I 42.5 R is provided as follows: “I” designates the initial type based on gypsum content (SO<sub>3</sub>), with a stipulated range between 1.5% and 3.5–4.0% for high-strength unblended cements. The numerical value “42.5” signifies the strength class, aligning with the minimum standard compressive strength. Lastly, the letter “R” designates the class associated with rapid early-age strength.

Table 2 delineates the chemical composition of CEM I 42.5 R, with the analysis conducted following the procedures outlined in [36].

**Table 2.** Mass fraction content of CEM I 42.5 R, wt%.

SiO <sub>2</sub>	Al <sub>2</sub> O <sub>3</sub>	Fe <sub>2</sub> O <sub>3</sub>	CaO	MgO	Na <sub>2</sub> O	K <sub>2</sub> O	SO <sub>3</sub>	Other Impurities
22.10	3.85	4.76	62.99	3.55	0.75	0.7	0.42	0.88

To validate the adherence of the chosen binder to established norms and requirements, several tests were conducted, utilizing methods specified in standards [28,29]. The results allowed for the determination of the following parameters:

- (1) Grinding fineness, using a sieve retention method [28] with a 0.08 mm sieve. For the tested binder, this amounted to 92.9%.
- (2) The standard consistency of cement paste and its setting time, using a Vicat apparatus needle method [29]. The standard consistency of cement paste was 26.8% by weight of cement. The beginning of setting [29] emerged after 2 h and 4 min, while the completion of setting occurred after 4 h and 24 min from the moment of mixing. These obtained parameters align with the stipulations in [15,16].

The fine aggregate utilized in the study was sourced from the manufacturer Mark, LLP, located in the Almaty region, Kazakhstan. This aggregate meets the specifications outlined in standard [21]. Table 3 provides an overview of the characteristics of the fine aggregate (sand) employed in the study.

To achieve desirable properties in concrete mix and concrete, it is imperative to utilize sand with a minimal presence of dust-like inclusions, not exceeding 1.5%. The examined sand exhibited a content of dust and clay inclusions of 1.38%. Additionally, the modulus of

coarseness for the investigated sand was 2.5. These values fall within the acceptable range for the use of the studied aggregate in heavy SCC, as specified in [21].

**Table 3.** Characteristics of sand.

Group of Sand	Grain Size, mm	Total Residue on Sieve No. 063, %	Content of Dust and Clay Inclusions, %	Quantity per 1 m <sup>3</sup> of Heavy SCC, kg
Coarse	2.5	64.1	1.38	800–1000

According to the guidelines of [37], the attainment of satisfactory characteristics in a mixture of heavy concrete necessitates that the total residues on the control sieves during the sieving of coarse aggregate (crushed stone and gravel) fractions 5–10 mm, 10–15 mm, 10–20 mm, 15–20 mm, 20–40 mm, and 40–80 mm, and the mixture of fractions 5–20 mm, correspond to the values delineated in Table 4, where *d* and *D* represent the smallest and largest nominal grain sizes, in millimeters.

**Table 4.** Recommended sieving rates for coarse aggregate [37] \*.

Diameter of Apertures in Control Sieves, mm	Total Residues Retained on Sieves, % by Weight
<i>D</i>	From 90 to 100
0.5( <i>d</i> + <i>D</i> )	From 30 to 60
<i>D</i>	Up to 10
1.25 <i>D</i>	Up to 0.5

\* For crushed stone and gravel fractions ranging from 5 to 10 mm, as well as a mixture of fractions spanning 5–20 mm, an additional criterion is applied: lower sieves with a mesh size of 2.5 mm (or 1.25 mm). The total residue on these lower sieves is expected to range from 95% to 100%. Alternatively, with mutual agreement between the manufacturer and the consumer, the production of crushed stone and gravel is permissible with a complete residue on a sieve of 0.5(*d* + *D*) falling within the range of 30% to 80% by weight, as specified in [37].

The coarse aggregate employed in the study consisted of crushed stone fractions of 5–10 mm and 10–20 mm, sourced from Kentas, LLP (Almaty, Kazakhstan). This aggregate complies with the specifications outlined in standard [22].

Table 5 shows detailed properties of the utilized coarse aggregate (crushed stone).

**Table 5.** Characteristics of coarse aggregate.

Grain Size, mm	Total Residue on Sieve of 0.5 ( <i>d</i> + <i>D</i> ), % (Norm Is 30–60)	Total Residue on Sieve of 1.25 <i>D</i> , % (Norm Is Less Than 0.5)	Quantity per 1 m <sup>3</sup> of Heavy SCC, kg
5–10	55.77	0.44	200–400
10–20	54.31	0.37	500–700

Table 6 presents the attributes of the microfiller (microsilica MC-95) from Tau-Ken Temir, LLP (Karaganda, Kazakhstan), utilized following the specifications in [23].

**Table 6.** Characteristics of microsilica [38].

Brand	Mass Fraction of Active SiO <sub>2</sub> , % by Weight, Not Less Than 95%	Quantity per 1 m <sup>3</sup> of Heavy SCC, kg
MC-95	96.85	up to 50

Microsilica comprises spherical particles with a diameter of 0.1 microns. The bulk density of microsilica falls within the range of 150 to 250 kg/m<sup>3</sup>. In terms of chemical composition, microsilica predominantly consists of non-crystalline silica, with a content typically exceeding 85% and reaching up to 98%. According to information from Tau

Ken Temir LLP (Karaganda, Kazakhstan) [38], microsilica possesses a specific surface area of 3980 cm<sup>2</sup>/g.

Table 7 shows the chemical composition of microsilica, as per the specifications outlined in [38].

**Table 7.** Chemical composition of microsilica MC-95, wt% [38].

SiO <sub>2</sub>	C	Water	Fe <sub>2</sub> O <sub>3</sub>	Al <sub>2</sub> O <sub>3</sub>	CaO	pH	ρ, g/cm <sup>3</sup>	Oth. imp.
96.85	1.31	1.07	0.07	0.24	0.46	7.89	0.44	1.68

Examination of the chemical composition provided by the manufacturer, when juxtaposed with the established quality standards for microsilica [23], indicates that the oxide content within the microsilica composition is adequate to yield satisfactory results in terms of achieving the specified objectives.

Based on the experience described in [39], opoka of the Shipovskoye deposit of the West Kazakhstan region was accepted as the next microfiller. Opal-chalcedony opoka of this deposit is composed mostly of amorphous silica, provided in the form of globules and spicules of marine sponges, radiolarians, shells, etc. Opoka mined from the Shipovskoye deposit is characterized by the presence of amorphous silica. Characteristics of the utilized opoka are given in Table 8.

**Table 8.** Characteristics of opoka from the Shipovskoye deposit [39].

Indicator	Indicator Value		
	Minimum	Maximum	Average
Specific gravity, N/m <sup>3</sup>	22.27 × 10 <sup>3</sup>	24.13 × 10 <sup>3</sup>	23.15 × 10 <sup>3</sup>
Density (in piece), kg/m <sup>3</sup>	1050	1665	1240
Water absorption, %	15.34	41.00	25.00
Compressive strength, MPa, in following conditions:			
Dry	6.239	14.09	10.16
Water-saturated	11.47	44.9	28.19
Frozen	25	37	31

Opoka derived from the Shipovskoye deposit has the chemical composition shown in Table 9.

**Table 9.** Chemical composition of opoka from the Shipovskoye deposit, wt% [39].

SiO <sub>2</sub>	Al <sub>2</sub> O <sub>3</sub>	Fe <sub>2</sub> O <sub>3</sub>	CaO	MgO	SO <sub>3</sub>
87.02	10.58	3.84	4.73	2.45	1.90

The chemical composition of opoka from the Shipovskoye deposit, when compared with the findings presented in [39], indicates that the content of basic oxides within the opoka's composition is sufficient to achieve the specified objectives. The opoka selected for testing underwent pre-milling to attain a specific surface of 1700–1850 cm<sup>2</sup>/g, using a laboratory ball mill BS BALLMILL-II (Zhengzhou TCH Instrument Co., Ltd., Henan, China) with a rotation range of up to 200 rpm.

As recommended in [7], metakaolin from Plast-Rifey, LLC, located in the city of Plast, Chelyabinsk region, Russia, was employed as the third mineral filler. The mineralogical composition of metakaolin, according to the manufacturer's data [40], is primarily characterized by fully amorphized kaolinite (90–93%), with a minor presence of crystalline phases represented by relict mica (2.5–3.0%) and quartz (4–5%). Crystalline neoplasms, such as

mullite and cristobalite, are virtually absent. The chemical composition of metakaolin is shown in Table 10.

**Table 10.** Chemical composition of metakaolin, wt% [40].

Al <sub>2</sub> O <sub>3</sub>	SiO <sub>2</sub>	Fe <sub>2</sub> O <sub>3</sub>	TiO <sub>2</sub>	K <sub>2</sub> O	Na <sub>2</sub> O	CaO	Oth. imp.
42.5	53.5	0.6	0.4	0.9	0.05	0.15	up to 1.5

Metakaolin stands out from microsilica, primarily due to its chemical composition. Unlike microsilica, metakaolin is characterized by a nearly equal mixture of active silica and alumina, making it an aluminosilicate pozzolan, rather than a silicate. This distinction, coupled with the utilization of highly efficient plasticizers, enables a substantial reduction in cement content in concrete compositions. This is particularly advantageous in concrete applications with heightened demands for water and frost resistance. Evidence [41] shows that at a dosage of just 2%, Portland cement with metakaolin already significantly increases the water resistance of resulting composition. According to [40], the aluminate component of metakaolin can actively interact with the gypsum contained in Portland cement or added specially to cement compositions.

Based on data from previously conducted studies, described in [42], on SCC as a plasticizing additive, the polycarboxylate ester AR 122, produced by ARGP, LLP (Astana, Kazakhstan), was adopted.

Table 11 shows the characteristics of the chemical additive, specifically, the hyperplasticizer polycarboxylate PCE from ARGP, LLP (Astana, Kazakhstan), following the specifications outlined in [24].

**Table 11.** Characteristics of the hyperplasticizer PCE [42].

Brand	Criterion for Additive Effectiveness	Quantity per 1 m <sup>3</sup> of Heavy SCC, kg
AR 122	from P1 to P5	from 7 to 15

## 2.2. Selection of the SCC Reference Composition

The mix design process adhered to Prof. Okamura's method [25], considering that, while the water–cement ratio is conventionally fixed for achieving the required strength in typical concrete mixtures, the water–binder ratio takes precedence in SCC design. This emphasis arises from the sensitivity of SCC's self-compaction ability to the water–binder ratio. Unlike in conventional concrete, where strength requirements determine the water–cement ratio, in SCC, the water–binder ratio is maintained at a low level that is sufficient to achieve the necessary strength for typical structures, unless reactive mineral admixtures are predominantly used. For SCC mortar, achieving both high viscosity and deformability is essential. This dual requirement is met by employing superplasticizers, which facilitate a low water-binding ratio, coupled with high deformability [43]. The ratio of coarse aggregate volume to its solid volume (G/Glim) for each concrete type is depicted in Figure 1. To mitigate interactions between coarse aggregate particles during concrete deformation, the packing degree of coarse aggregate in SCC is maintained at approximately 50%. Additionally, Figure 1 illustrates the volume ratios of fine aggregate to solid aggregate (S/Slim) in the mortar. The packing degree of fine aggregate in SCC mortar is around 60%, thereby limiting shear deformability during concrete deformation.

Subsequently, following the criteria proposed by Prof. Okamura, the quantity of coarse aggregate was determined. The proportion of coarse aggregate was established at 0.5 of coarse aggregate weight in relation to bulk density. For instance, at a density of 1500 kg/m<sup>3</sup> in a dry

compacted state, the coarse aggregate content would be calculated as  $1500 \times 0.5 = 750$  kg. In this scenario, the coarse aggregate consists of particles with a size exceeding 4.75 mm.

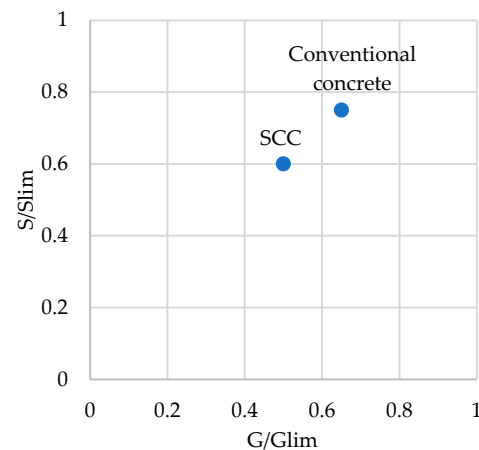


**Figure 1.** Aggregate compaction degree [25].

The content of fine aggregate was set at 0.6 in relation to bulk density. Material with a grain size between 4.75 and 0.09 mm was accepted as a fine aggregate. The content of fine aggregate was  $1500 \times 0.6 = 900$  kg.

To further characterize the materials used in the SCC, such as the binder, sand, and superplasticizer, tests were carried out to determine the viscosity of the mortar in the form of flow time from the funnel. Tests were also performed on the deformability properties of the mortar by determining the cone spread.

### 2.3. Input of Mineral Additives

Several tests were carried out to determine the slump flow rate at the initial ratio of water and binder, equal to 0.4, and with 1% superplasticizer in relation to the amount of binder, with various mineral additive dosages. The task was to obtain a mixture of water, binder, and superplasticizer that, in the test, would show a slump flow [30] of 244–246 mm and a flow time through the funnel of 9–11 s [25]. Further, a complete calculation of the concrete mixture components was performed, and laboratory testing of the rheological properties of the obtained compositions was carried out to prove their successful selection. Generalized data on the mortar's rheological properties with the use of different amounts of 3 mineral fillers are shown in Tables 12–14.

Tables 12–14 show that to obtain the required rheological properties when using opoka, it is necessary to replace 5% of the cement. A further increase in the amount of opoka reduces the blurring and flow time through the funnel, which can be explained by the high water consumption of opoka. This is because opoka is a sedimentary rock consisting mainly of the remains of siliceous organisms, due to which its structure has a large volume of micropores, which gives a large specific volume of voids capable of absorbing and retaining water.

To achieve the required performance when using metakaolin, it is necessary to replace 10% of the cement. When the amount of metakaolin is further increased, the performance also decreases. This can be explained by the fact that after firing, kaolin becomes very finely dispersed and acquires a large specific surface area ( $8000\text{--}15000\text{ cm}^2/\text{g}$ , according to Blaine), which contributes to the adsorption of a significant amount of water. The replacement of 15% of cement with microsilica seems to be the most effective in terms of achieving the lowest consumption of expensive hyperplasticizer, as it achieves the most effective utilization of ferroalloy production waste, while maintaining the necessary rheological properties.

**Table 12.** The effect of the amount of added microsilica on the rheology of the cement–sand mixture.

No.	Core Composition *	Cement, kg	Microsilica Quantity in Cement Weight, %	Microsilica Quantity in Cement Weight, kg	Quantity of Superplasticizer, kg	Slump Flow, mm	Flow Time, s
1	Sand—900 kg, Water—0.4 of cement	600	0	0	6	265	7
2		570	5	30	6	261	8
3		540	10	60	6	253	9
4		510	15	90	6	245	10
5		480	20	120	6	237	12
6		420	30	180	6	231	14

\* All data are based on the quantity of components per 1 m<sup>3</sup> of concrete or mortar mixture.

**Table 13.** The effect of the amount of added opoka on the rheology of the cement–sand mixture.

No.	Core Composition *	Cement, kg	Opoka Quantity in Cement Weight, %	Opoka Quantity in Cement Weight, kg	Quantity of Superplasticizer, kg	Slump Flow, mm	Flow Time, s
1	Sand—900 kg, Water—0.4 of cement	600	0	0	6	265	7
2		570	5	30	6	246	9
3		540	10	60	6	232	12
4		510	15	90	6	227	14
5		480	20	120	6	213	17
6		420	30	180	6	205	20

\* All data are based on the quantity of components per 1 m<sup>3</sup> of concrete or mortar mixture.

**Table 14.** The effect of metakaolin addition quantity on the rheology of the cement–sand mixture.

No.	Core Composition *	Cement, kg	Metakaolin Quantity in Cement Weight, %	Metakaolin Quantity in Cement Weight, kg	Quantity of Superplasticizer, kg	Slump Flow, mm	Flow Time, s
1	Sand—900 kg, Water—0.4 of cement	600	0	0	6	265	7
2		570	5	30	6	251	8
3		540	10	60	6	245	9
4		510	15	90	6	240	11
5		480	20	120	6	232	13
6		420	30	180	6	225	15

\* All data are based on the quantity of components per 1 m<sup>3</sup> of concrete or mortar mixture.

Further, from mortar mixtures showing the necessary values of slump flow and funnel flow time, samples were molded, which were tested for compressive strength, according to the method described in [32], after 1 day and 28 days.

#### 2.4. Study of the Macrostructure and Microstructure of Samples

Macroscopic observations of the mortar samples were conducted visually before microscopic analysis (i.e., SEM), following common laboratory practice. The surface condition, homogeneity, and presence of visible defects, such as cracks or pores, were assessed. Further, for examination of the material's microstructure [17], slices of mortar specimens at the 28-day mark were scrutinized utilizing a German ZEISS Axio Vert.A1 electron microscope through reflective photography with a magnification of  $\times 500$ . The SEM observations were carried out using secondary electron imaging mode at an accelerating voltage of 15 kV and a working distance of 10 mm. Furthermore, to evaluate the impact of mineral additives on the phase composition of cement paste hydration products, X-ray diffraction (XRD) [18] was employed. This analysis was conducted using the D2PHASER powder diffractometer (Bruker Corporation, Billerica, MA, USA), with Cu-K $\alpha$  radiation ( $\lambda = 1.5406 \text{ \AA}$ ), a step size of  $0.02^\circ 2\theta$ , a scanning range from  $5^\circ$  to  $70^\circ 2\theta$ , and a scan speed of  $1^\circ/\text{min}$ .

### 2.5. Determination of SCC Rheological Characteristics

During this phase, the samples underwent comprehensive testing to ascertain the rheological properties of the SCC mixture and the primary performance and deformation characteristics of the hardened concrete. These assessments were conducted to thoroughly investigate the functioning of the cement–mineral admixture system and its impact on the properties of this specific type of concrete [44].

#### 2.5.1. Determination of the Deformability of SCC

The deformability of the SCC mixture was initially assessed by examining the cone spreading. According to the method described in [30], the cone and a metal sheet were wetted, and the cone was then positioned on the metal sheet with its smaller base touching the sheet's surface. The concrete mixture was poured until the cone was completely filled in a single operation. After the cone was lifted for 5–7 s and the mixture came to a complete halt, the two largest spalling diameters were measured. The test result was determined as the arithmetic mean of the two largest spread diameters. Based on [32], SCCs were categorized into three classes according to their workability index, denoted as SF1, SF2, and SF3, with corresponding slump flows of 550–650 mm, 660–750 mm, and 760–850 mm, respectively.

According to [26], for the utilization of SCC in large-scale and reinforced structures, ensuring the necessary surface quality requires the mixture to align with the SF2 class in terms of workability. Additionally, the optimal cone spreading for this class is within the range of 680–750 mm.

The viscosity class of SCC was ascertained through flow time measurement in a V-funnel, following the guidelines specified in the normative document [31] (V-funnel test). After cleaning and wetting the V-funnel [31] and the gate, the gate was closed. The concrete mixture was poured into the funnel in one go, and then the excess concrete mixture was removed flush with the top edge of the funnel. A container for draining was placed under the funnel. After  $10 \pm 2$  s from the time the funnel was filled, the gate was opened. The time up to 0.1 s from the opening of the stopper to the complete flow of the concrete mixture out of the funnel was measured. The time taken for the mixture to flow out of the funnel was the result of the test.

#### 2.5.2. Determination of the Viscosity of SCC

According to [32], SCC is classified into two classes according to its viscosity index: VF1 and VF2, with flow times of  $\leq 8$  and 9–25 s, respectively. As defined by [26], the optimal time of flow from the V-shaped funnel is 8–14 s, which corresponds to the viscosity index VF2. At this viscosity index, the flow of the SCC mixture is uninterrupted and smooth, and the molded samples have the desired surface quality. Viscosity also affects the segregation performance of the mixture. An increased viscosity index can signal an increased water–cement ratio, which subsequently leads to the segregation of the mixture in the structure.

### 2.6. Selection of SCC Reference Composition

Further, based on the obtained data on the deformability, viscosity, and compressive strength of the mortar compositions, according to the selection principle of [25–27], the optimal compositions of SCC with three types of mineral fillers were calculated, the summary data of which are presented in Table 15.

**Table 15.** SCC compositions.

No.	W/C	Cement, kg/m <sup>3</sup>	Mineral Additive kg/m <sup>3</sup>	Sand, kg/m <sup>3</sup>	Crushed Stone, 5–10 mm, kg/m <sup>3</sup>	Crushed Stone, 10–20 mm, kg/m <sup>3</sup>	Additive, kg/m <sup>3</sup>
1 (reference)	0.4	600	0	900	488	262	6
2 (with microsilica)	0.4	510	90	900	488	262	6
3 (with opoka)	0.4	570	30	900	488	262	6
4 (with metakaolin)	0.4	540	60	900	488	262	6

### 2.7. Verification of Operational Reliability of SCC

Verification of the operational reliability of SCC was performed through a series of fundamental tests to assess durability [35] and persistence [30,31].

## 3. Results and Discussion

### 3.1. Results of Tests for Rheological Properties

The results of the deformability tests of the SCC mixtures by determining slump flow are presented in Table 16 below.

**Table 16.** The slump flow of the obtained SCC compositions.

No.	Slump Flow, mm	Class
1 (reference)	640	SF1
2 (with microsilica)	710	SF2
3 (with opoka)	630	SF1
4 (with metakaolin)	680	SF2

The results show that the compositions with microsilica and metakaolin have higher rates of spreading than the reference composition, since their higher specific surface area of 4000–4500 g/cm<sup>2</sup> contributes to the creation of a microcapillary structure in the cement paste, and significantly reduces the volume of micropores at relatively low dosages of plasticizer; this effect is more pronounced under lower cement consumption. In the process of concrete hardening, the degree of hydration of the cement binder increases in the early stages. When introducing mineral fillers into the mixture, there is a significant additional interface surface, “filler–water”, which is immediately reflected in the rheological efficiency of the cement–mineral additive system [45]. Similar effects were reported by [4,46], who noted that the use of fine pozzolanic materials improves the deformability of SCC by refining the particle structure and promoting a denser paste matrix. Additionally, the enhanced early hydration kinetics, as discussed by [15], contribute to better flowability, due to the accelerated formation of hydration products at the filler–water interface.

The results of viscosity testing of the SCC mixtures by measuring the flow time through the V-funnel are presented in Table 17 below.

**Table 17.** The viscosity of the obtained SCC compositions.

No.	Flow Time, s	Class
1 (reference)	6	VF1
2 (with microsilica)	12	VF2
3 (with opoka)	8	VF1
4 (with metakaolin)	15	VF2

The results show that the compositions with the inclusion of microsilica and metakaolin have higher viscosity values than the reference composition. Apparently,

this is connected both with the effect of microfilling, which involves a range of different effects of mineral additives on the concrete mixture, and with the activity of these additives themselves, which results in the reduction of calcium hydroxide  $\text{Ca}(\text{OH})_2$  and an increase in the degree of hydration of the cement system [43]. Also, the introduction of mineral fillers increases the content of fine particles in the mixture and their concentration in the cement paste; this factor, as a result, improves the viscosity of the concrete mixture [43]. A comparable phenomenon was observed by [4], who found that mineral additives with a high specific surface area enhance the compactness of the microstructure and increase the resistance to flow. Additionally, refs. [46,47] emphasize that the pozzolanic activity of microsilica and metakaolin facilitates the rapid consumption of calcium hydroxide and accelerates the formation of hydration products, which, in turn, elevate the viscosity and improve the stability of the fresh concrete mix.

### 3.2. Results of Tests for Strength Properties

The results of compressive strength tests of mortar specimens with microsilica, opoka, and metakaolin at the ages of 1 day and 28 days are presented in Table 18.

**Table 18.** Strength of SCC samples with different mineral additives.

No.	Cement	Quantity of Filler, %	Quantity of Filler, kg	Strength Values, MPa (Age)							
				Microsilica		Opoka		Metakaolin		No Additives	
				1	28	1	28	1	28	1	28
1	600	0	0	-	-	-	-	-	-	11.2	37.7
2	570	5	30	-	-	11.5	38.1	-	-	-	-
3	540	10	60	-	-	-	-	12.5	41.5	-	-
4	510	15	90	12.8	40.7	-	-	-	-	-	-

Note: “-” means no value.

The strength characteristics of the mortar specimens show that the best effect is achieved when replacing part of the cement with 10–15% of microsilica and metakaolin. These results align well with previous findings of [12], emphasizing that metakaolin not only improves compressive strength, but also accelerates strength development, due to its high alumina content and amorphous structure. Similarly, ref. [9] notes that the use of highly reactive pozzolanic materials contributes to strength gain by refining the pore structure and increasing the degree of hydration.

### 3.3. Results of Microstructure Analysis

Figure 2 shows the macrostructure of the SCC mortar samples before the microstructure study.

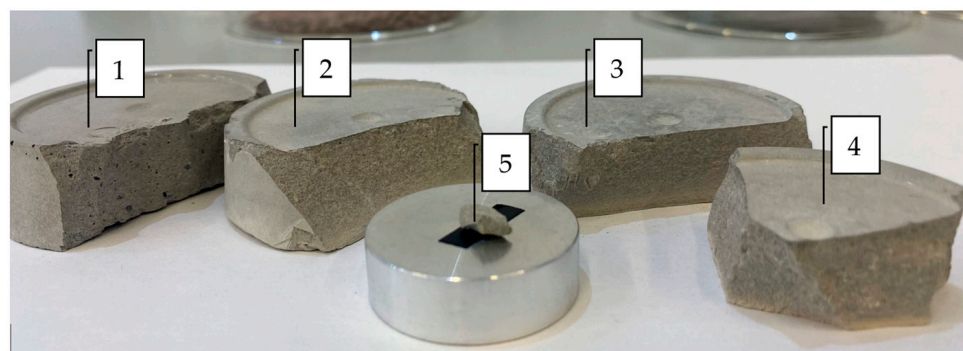


**Figure 2.** Macrostructure of SCC mortar samples: (1) without filler; (2) 5% opoka; (3) 10% metakaoline; (4) 15% microsilica; (5) sample for SEM.

In Figure 2, it can be seen that sample 1, pure cement, has pores visible to the naked eye, indicating a less dense and potentially more permeable structure. In contrast, all samples modified with mineral additives (opoka, metakaolin, and microsilica) exhibit visually denser and more homogeneous surfaces without noticeable defects, suggesting improved compaction and internal structure. Particularly, the sample with 15% microsilica appears to have the smoothest surface texture, which reflects the effectiveness of microsilica in filling the microvoids of the cement paste. The sample with 10% metakaolin also demonstrates good surface integrity, consistent with the known microfilling and pozzolanic properties of metakaolin [12,47]. The observed improvements in macrostructure correspond to the expected benefits of using finely dispersed mineral fillers, which enhance particle packing and reduce the porosity of the cementitious matrix [48,49]. The figure also shows a broken piece of mortar ready for further microscopic analysis.

Figure 3 shows an image of the fracture microstructure of the reference specimen made from pure cement.

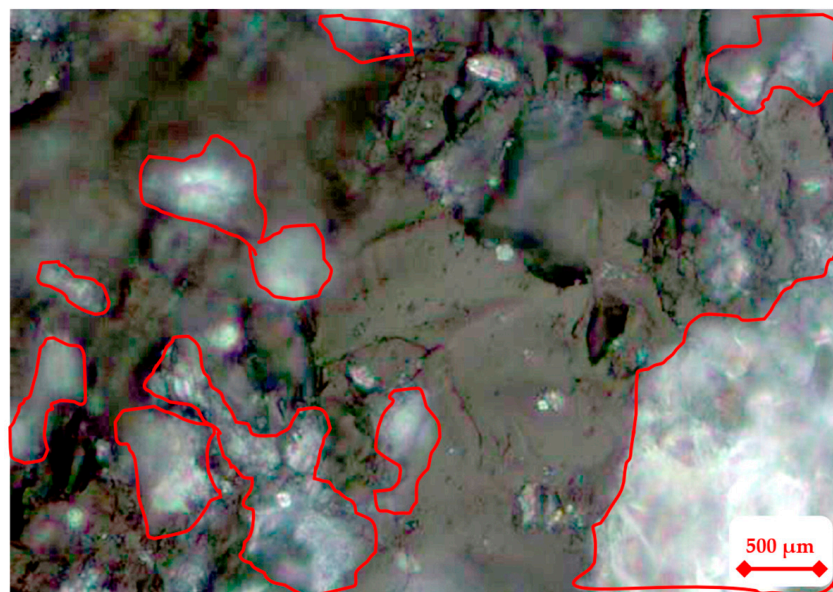


**Figure 3.** Microstructure of SCC made from pure cement (magnification of 500  $\mu\text{m}$ ).

The image shows that the structure of the cement paste without additives is heterogeneous, has block-like characteristics, and is represented by weakly crystallized interlayers of highly basic metastable calcium hydrosilicates ( $\text{CaO}\cdot\text{SiO}_2\cdot\text{H}_2\text{O}\cdot(\text{CaO}/\text{SiO}_2 > 1.5)$  or  $\text{C}_2\text{SH}_2$  (delineated in red in Figure 3); these neoplasms with increased basicity have a tendency to coagulate [45], containing water molecules held by adsorption forces. The evaporation of water adsorbed and located in the crystal lattice is accompanied by shrinkage of the system, which is in agreement with the suggestions of the authors of [45].

Figure 4 shows an image of the fracture microstructure of the sample containing opoka.

The image shows that the hydraulic activity of opal-chalcedony opoka is caused by the chemical interaction of the amorphous silica included in its composition with lime, which is formed during cement hydration as a result of hydrolysis of  $3\text{CaO}\cdot\text{SiO}_2$ , according to the formula  $2(3\text{CaO}\cdot\text{SiO}_2) + 6\text{H}_2\text{O} = 3\text{CaO}\cdot 2\text{SiO}_2\cdot 3\text{H}_2\text{O} + 3\text{Ca}(\text{OH})_2$  (delineated in red in Figure 4). The interaction products are low-basicity C-S-H type calcium hydrosilicates (B),  $3\text{CaO}\cdot\text{Al}_2\text{O}_3\cdot 6\text{H}_2\text{O}$  hydroaluminates, and  $\text{CaO}\cdot\text{Fe}_2\text{O}_3\cdot n\text{H}_2\text{O}$  calcium hydroferrites. The neoplasms are usually in the form of thin fibers, plates, and irregularly shaped petals [50].

Figure 5 shows an image of the fracture microstructure of a sample containing metakaolin.

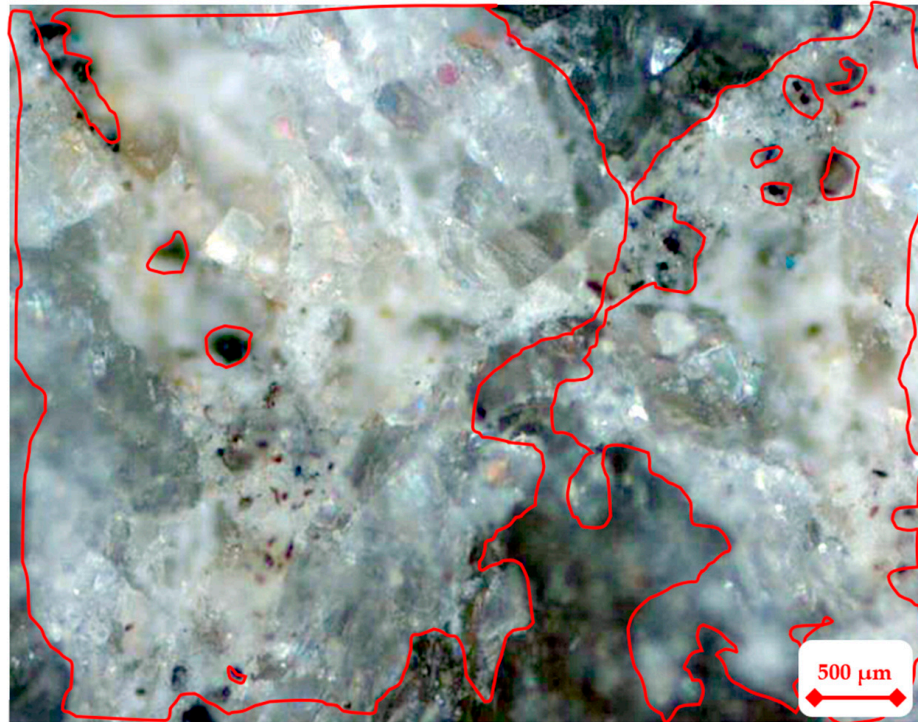


**Figure 4.** Microstructure of SCC with opoka (magnification of 500 μm).

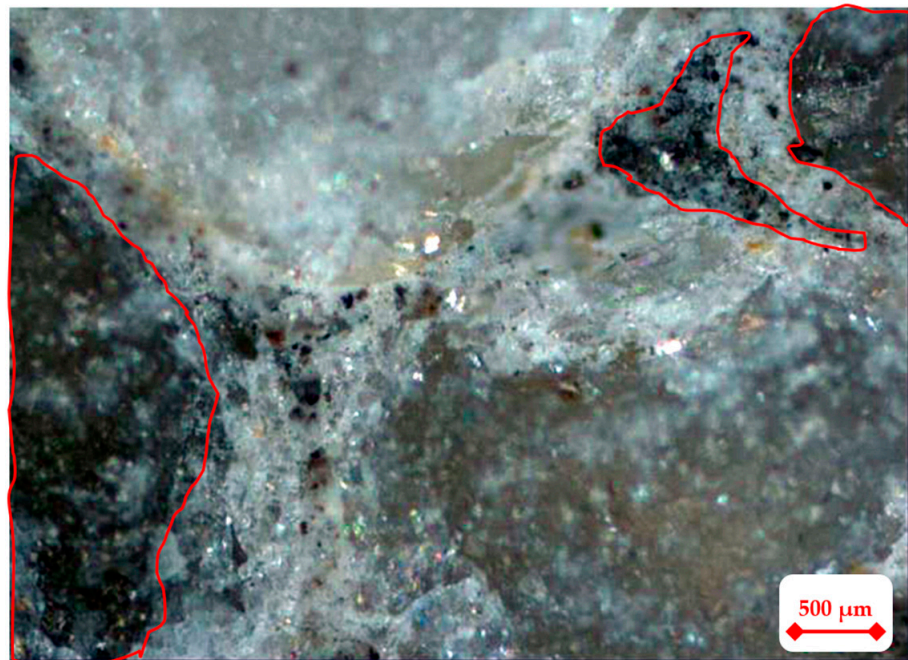


**Figure 5.** Microstructure of SCC on metakaolin (magnification of 500 μm).

The image shows that the interaction of active kaolinite anhydrite—amorphized metakaolinite ( $\text{Al}_2\text{O}_3 \cdot 2\text{SiO}_2$ ) and calcium oxide hydrate  $\text{Ca}(\text{OH})_2$  produces helenite hydrate  $2\text{CaO} \cdot \text{Al}_2\text{O}_3 \cdot \text{SiO}_2 \cdot 8\text{H}_2\text{O}$  and a low-basicity calcium hydrosilicate of  $\text{CSH}(\text{B}) \cdot (\text{CaO}/\text{SiO}_2 < 1.5)$  with a ratio of 0.8 to 1.5, depending on the concentration of CaO in aqueous solution [7]. Areas that have not been hydrated are delineated in red.

Figure 6 shows an image of the fracture microstructure of the sample containing microsilica MC-95.

The photo shows that the cement paste with the MC-95 additive has a more pronounced homogeneous structure than the cement paste without additives. The reaction between clinker hydration products and active microsilica is essentially a process of interaction of  $\text{Ca}(\text{OH})_2$  with the active  $\text{SiO}_2$  included in the composition of microsilica, which creates conditions for the formation of a structure with the densest packing of crystals, consisting mainly of low-basicity calcium silicate hydroxides of type CSH(B), for example,  $(\text{Ca}_5(\text{OH})_2\text{Si}_6\text{O}_{16}\cdot 4\text{H}_2\text{O}\cdot (\text{CaO}/\text{SiO}_2 < 1.5))$ , which confirms the theory presented in [46]. Areas that have not been hydrated are delineated in red.

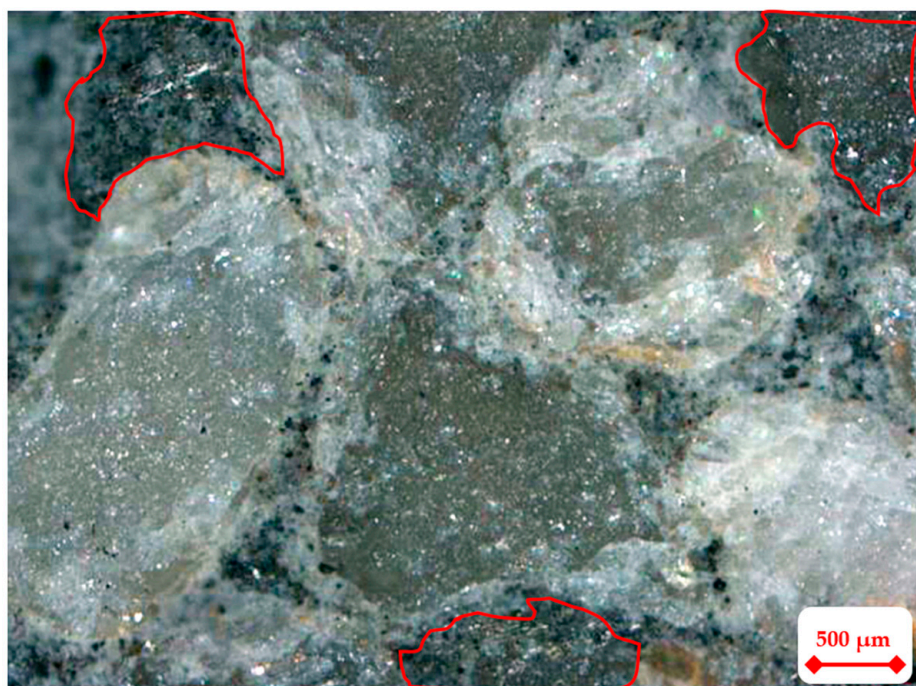


**Figure 6.** Microstructure of SCC with microsilica (magnification of 500  $\mu\text{m}$ ).

The microstructural analysis of the SCC samples revealed notable differences between the reference composition and those modified with mineral fillers. The reference sample, made with pure cement, exhibited a heterogeneous structure with poorly crystallized, highly basic calcium hydrosilicates ( $\text{C}_2\text{SH}_2$ ), prone to coagulation and shrinkage upon water loss, consistent with the observations described by [45]. In contrast, the sample with opoka showed formation of low-basicity C-S-H phases, hydroaluminates, and hydroferrites as a result of the pozzolanic reaction between the amorphous silica of opoka and lime, supporting findings reported by [4].

The microstructure of the metakaolin-modified SCC demonstrated the development of helenite hydrates and low-basicity calcium hydrosilicates (CSH(B)), indicating a more stable and densely packed matrix, in agreement with [7], who noted the beneficial role of aluminosilicates in accelerating hydration and improving microstructural homogeneity. Similarly, the sample containing microsilica showed the most homogeneous and dense microstructure, with well-developed low-basicity calcium silicate hydrates, confirming the microfilling and pozzolanic effects described by [46].

#### 3.4. Results of XRD Analysis

As a result of the evaluation of the phase composition of neoplasms using the XRD method with a D2PHASER diffractometer (Bruker Corporation, Billerica, MA, USA), the following data were obtained (Figures 7–10).

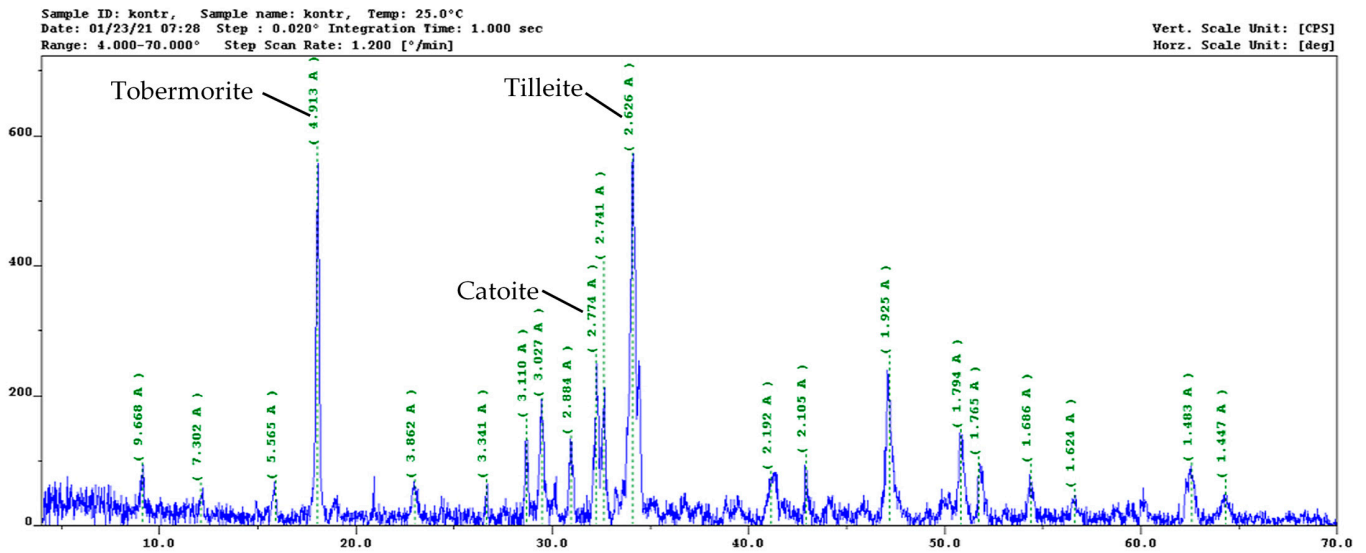


Figure 7. Reference sample without mineral additive.

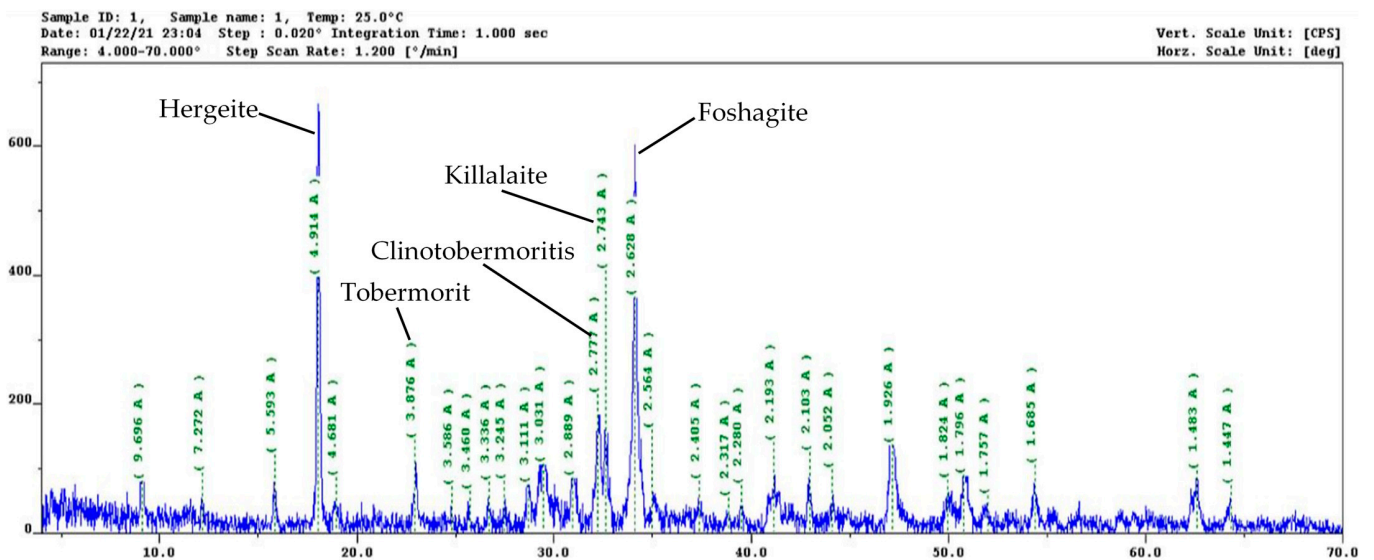


Figure 8. Sample with replacement of part of cement with microsilica.

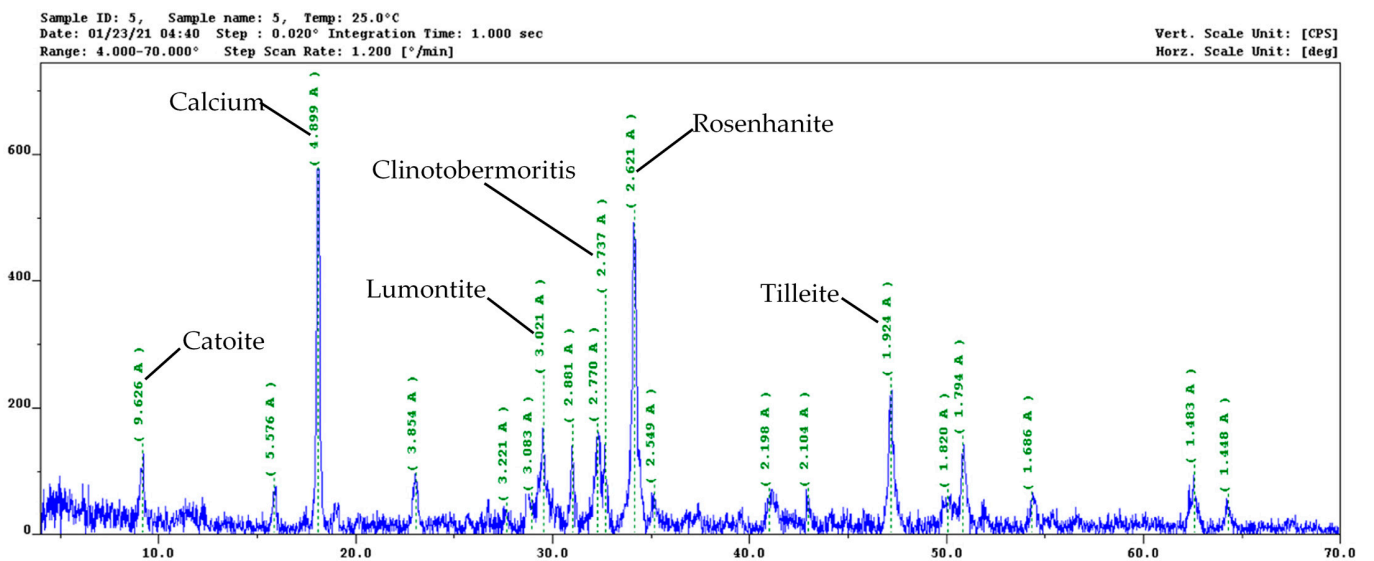


Figure 9. Sample with replacement of part of cement with opoka.

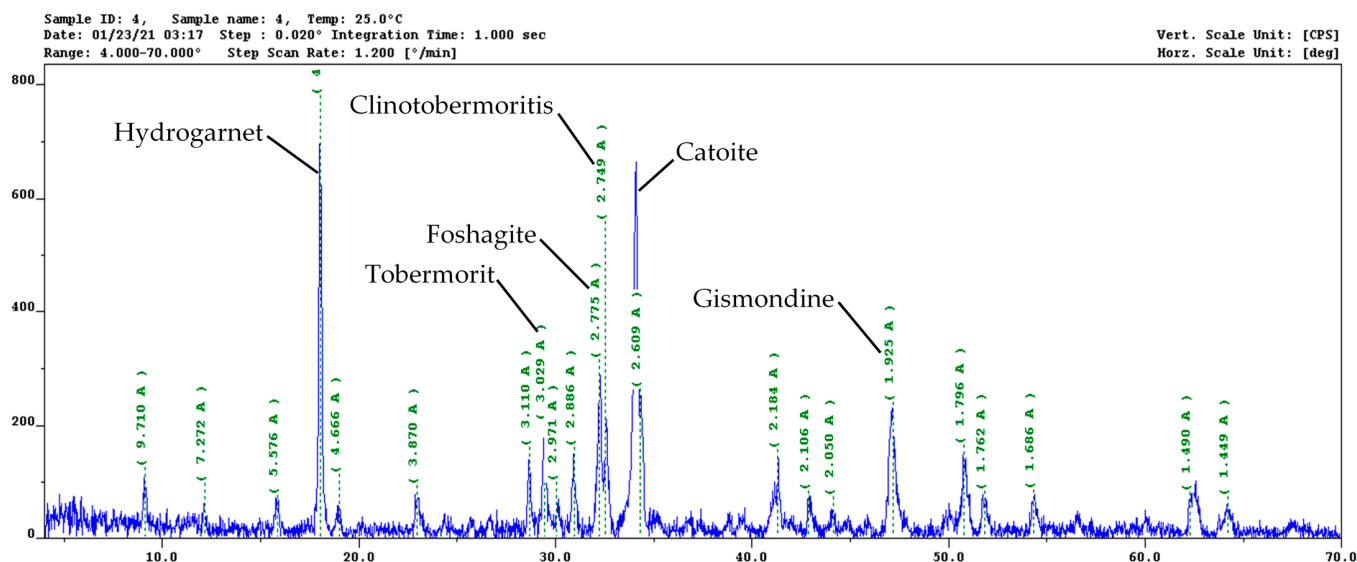


Figure 10. Sample with replacement of part of cement with metakaolin.

Using the software DIFFRAC.EVA V.5.1.0.5 and DIFFRAC.TOPAS V.4.2, the obtained diffractograms were analyzed, and the results are shown in Tables 19 and 20.

Table 19. Phase composition of cement paste at age of 28 days of normal hardening.

No.	Cement Paste	Phase Composition of Cement Paste, %			
		C <sub>3</sub> S	C <sub>2</sub> S	Ca(OH) <sub>2</sub>	Hydration Degree
1	Reference	19.6	8.8	11.6	70
2	Portland cement + microsilica	12.7	6.5	18.8	84
3	Portland cement + opoka	15.2	7.2	14.3	78
4	Portland cement + metakaolin	12.6	6.4	18.5	82

Table 20. The calcium hydrosilicate content in the investigated samples of modified cement paste at the age of 28 days of water curing.

Sample	Notation Designation	Calcium Hydrosilicates
Reference	1	Tobermorite Ca <sub>2</sub> H <sub>3</sub> O <sub>11</sub> Si <sub>3</sub> Catoite Al <sub>2</sub> Ca <sub>3</sub> H <sub>12</sub> O <sub>12</sub> Si <sub>3</sub> Tilleite C <sub>2</sub> Ca <sub>5</sub> O <sub>13</sub> Si <sub>2</sub>
Portland cement + microsilica	2	Hergeite Ca <sub>5</sub> H <sub>2</sub> K <sub>2</sub> O <sub>25</sub> S <sub>6</sub> Tobermorite Ca <sub>2</sub> H <sub>3</sub> O <sub>11</sub> Si <sub>3</sub> Clinotobermoritis Ca <sub>5</sub> H <sub>8</sub> O <sub>21</sub> Si <sub>6</sub> Killalaita Ca <sub>2</sub> H <sub>6</sub> O <sub>11</sub> Si <sub>3</sub> Foshagite Ca <sub>4</sub> H <sub>2</sub> O <sub>11</sub> Si <sub>3</sub>
Portland cement + opoka	3	Catoite Al <sub>2</sub> Ca <sub>3</sub> H <sub>12</sub> O <sub>12</sub> Si <sub>3</sub> Calcium hydroferrite 4CaOFe <sub>2</sub> O <sub>3</sub> n+3H <sub>2</sub> O Lumontite Al <sub>4</sub> Ca <sub>2</sub> H <sub>18</sub> O <sub>33</sub> Si <sub>8</sub> Clinotobermoritis Ca <sub>5</sub> H <sub>8</sub> O <sub>21</sub> Si <sub>6</sub> Rosenhanite Ca <sub>3</sub> H <sub>2</sub> 10Si <sub>3</sub> Tilleite C <sub>2</sub> Ca <sub>5</sub> O <sub>13</sub> Si <sub>2</sub>
Portland cement + metakaolin	4	Hydrogarnet Al <sub>3,5</sub> Ca <sub>3</sub> H <sub>9,875</sub> O <sub>2</sub> Tobermorite Ca <sub>2</sub> H <sub>3</sub> O <sub>11</sub> Si <sub>3</sub> Foshagite Ca <sub>4</sub> H <sub>2</sub> O <sub>11</sub> Si <sub>3</sub> Clinotobermoritis Ca <sub>5</sub> H <sub>8</sub> O <sub>21</sub> Si <sub>6</sub> Catoite Al <sub>2</sub> Ca <sub>3</sub> H <sub>12</sub> O <sub>12</sub> Si <sub>3</sub> Gismondine Al <sub>2</sub> CaH <sub>8,66</sub> O <sub>12,303</sub> Si <sub>2</sub>

Analysis of phase composition showed that replacing part of the cement with the mineral additives microsilica and metakaolin (compositions 2 and 4) led to intensification of the

hydration process and binding of the calcium hydroxide ( $\text{Ca}(\text{OH})_2$ ) formed by microsilica and metakaolin, a decrease in the content of  $\text{C}_3\text{S}$  and  $\text{C}_2\text{S}$  in comparison with composition 1, and an increase in the degree of hydration from 70 to 82%, respectively. Replacing part of the cement with opoka (composition 3) showed intermediate results between those of the reference composition 1 and compositions 2 and 4, along with a decrease in the amount of the minerals ( $\text{C}_3\text{S}$ ) and ( $\text{C}_2\text{S}$ ), as well as compaction and strengthening of the cement paste structure [47].

The analysis of diffractograms of samples confirmed the theory stated in [4,44] about the formation of a large number of highly stable low-basicity hydrosilicates and calcium hydroaluminates in samples with the addition of active minerals. A more interesting observation is that compared to the three low-basicity calcium hydrosilicates formed in reference sample 1, pure cement, all samples with the addition of active minerals, samples 2, 3, and 4, formed 5–6 of these stable compounds (Table 17). This once again indicates intensification of the hydration processes of cement paste minerals and intensive crystallization of the colloidal system in the presence of active  $\text{SiO}_2$  and  $\text{Al}_2\text{O}_3 \cdot 2\text{SiO}_2$ . The increased quantity of low-basicity calcium hydrosilicates, such as tobermorite and clinotobermorite, in samples with microsilica and metakaolin is consistent with the findings of [46], the authors of which demonstrated that the addition of highly reactive silica phases promotes the formation of more stable and finely distributed hydration products. Moreover, the appearance of phases like hydrogarnet and gismondine in the modified systems corresponds with the results reported by [12], highlighting that active aluminosilicate additives such as metakaolin not only accelerate cement hydration, but also contribute to the development of complex calcium-alumino-silicate hydrates (C-A-S-H), which further strengthen the cementitious matrix. Overall, the XRD analysis confirms that the use of active mineral additives significantly alters the phase assemblage, favoring the formation of stable crystalline hydrates, and thereby improving the structural integrity and long-term performance of SCC.

### 3.5. Results of Tests for Durability

The summarized results of the tests for the determination of the physical, mechanical, and operational properties of the SCC compositions (Table 15) are presented in Table 21.

**Table 21.** Performance properties of concretes.

No.	Frost Resistance, Cycles (F)	Volumetric Water Absorption, %	Shrinkage, %
1 (reference)	200	6.7	−0.25
2 (with microsilica)	300	4.9	−0.17
3 (with opoka)	250	6.5	−0.24
4 (with metakaolin)	300	4.8	−0.18

The test results of the concrete samples for frost resistance demonstrate a general trend of increasing frost resistance, from F200 for concrete samples without additives and containing pure cement, to F250 for samples with opoka addition and F300 for samples with the addition of microsilica and metakaolin, while the strength class remains consistent across all samples. It is also noteworthy that there is a reduction of up to 30% in the indicators of volumetric water absorption and a decrease in deformation shrinkage values by 0.07% for concrete samples with the addition of microsilica and metakaolin. This indicates agreement between the research results and theoretical assumptions regarding the emergence of additional crystallization centers and a reduction in the pore space in the concrete body, due to reactions of active pozzolanic additives (active microsilica  $\text{SiO}_2$ ). The binding process of  $\text{Ca}(\text{OH})_2$  by the active mineral additive  $\text{SiO}_2$  into a sparingly

soluble compound, calcium hydrosilicate, occurs according to the following equation:  $\text{Ca}(\text{OH})_2 + \text{SiO}_2 + m\text{H}_2\text{O} = \text{CaO} \cdot \text{SiO}_2 \cdot n\text{H}_2\text{O}$  [47].

Shrinkage cracks are also one of the most common problems encountered during the self-compacting concrete product curing process. Since SCC is a specific concrete with a higher volume content of cement paste, it was necessary to show that the use of mineral admixtures in SCC would reduce the risk of shrinkage cracking [1]. According to the measured shrinkage strains of self-compacting concrete using different types of mineral admixtures, it can be said that the use of mineral admixtures can reduce the shrinkage strains of cement paste by reducing the gel component of cement paste, which contains a large amount of adsorbed  $\text{H}_2\text{O}$  in its pores; this leads to a decrease in volume, which can be seen in electron microscopic analysis [46].

Further, at the manufacturing plant Temirbeton 1, LLP (Almaty, Kazakhstan), trial casting of the obtained self-compacting concrete with the addition of microsilica and metakaolin of class C30/35 was realized. The trial casting was carried out in a lego block foundation structure, FBS 160.40.80 (Figure 11). The essence of the research on the trial pouring consisted of comparison of the strength characteristics and surface quality of three types of concrete—ordinary cast concrete produced by Temirbeton-1; LLP with SF1 and VF1 slump flow and viscosity indices; SCC with the addition of microsilica, with SF2 and VF2 slump flow and viscosity indices; and SCC with metakaolin, with SF2 and VF2 slump flow and viscosity indices. According to the results of the casting, a report was drawn up, containing information about the molded products, the composition of the poured SCC, and the strength characteristics of the products at 3 days after casting, as well as at the ages of 7 and 28 days [51].



**Figure 11.** The upper product is made of SCC with silica fume, while below it, for comparison, is an identical product made of conventional concrete of the same strength class, produced without vibration compaction.

According to the results of production testing, the products poured from SCC with microsilica and metakaolin had the best surface (class A1) and higher strength characteristics than the ordinary SCC of the same class (Table 22).

The results of the production tests clearly show the importance of the rheological characteristics of the SCC mixture [52]. Products 1 and 3, molded from the experimental compositions with replacement of part of the cement with the mineral additives microsilica and metakaolin, show optimal values of deformability and viscosity, with surface quality A1 and an increase in strength by 20–25% compared to that of ordinary cast concrete without additives, for which we saw underconsolidation and partial delamination of the concrete mixture, with correspondingly lower indicators of surface quality and strength, agreeing with results obtained previously [14,53].

**Table 22.** The strength of the tested SCC compositions in the products poured at the factory.

No.	Concrete Type	Concrete Compressive Strength, MPa		
		3-Day	7-Day	28-Day
1	Ordinary cast-in-place concrete C30/35	21.2	29.8	35.4
2	SCC with microsilica C30/35	27.9	34.7	38.1
3	SCC with metakaolin C30/35	28.3	35.1	37.9

#### 4. Conclusions

According to the results of the tests carried out, the following can be assumed:

- The mixture with replacement of part of the cement with opal-chalcedony opoka has the least homogeneous structure, in which both calcium hydrosilicates and hydroaluminates and hydroferrites can be traced, which can be clearly seen in the images and XRD data. This inhomogeneity of the structure was corroborated during further tests on operational reliability, with opoka producing the lowest values out of the three mineral additives in the tests for frost resistance and water absorption, as well as negatively affecting the strength characteristics of the final conglomerate.
- A more homogeneous structure, characterized mainly by low-basicity calcium hydrosilicates of the CSH(B) type, as well as higher performance and strength, were shown in the compositions with the inclusion of microsilica and metakaolin. Apparently, these properties are connected both with the effect of microfilling, which involves a range of different effects of mineral additives on the concrete mixture, hardening concrete, and hardened concrete, and with the activity of the additives themselves, resulting in a reduction in calcium hydroxide  $\text{Ca}(\text{OH})_2$  and an increase in the degree of hydration.
- The addition of mineral fillers increased the content of fine particles in the mixture and their concentration in the cement dough, creating a microcapillary structure of cement paste and significantly reducing the volume of micropores, consequently reducing permeability. As hydration proceeds, capillary pores are gradually replaced by new formations, which leads to an increase in the volume of helium pores at the expense of a decrease in the volume of capillary pores. At the same time, both the total cumulative volume of pore space and the average pore volume decrease. As a result, this factor increased the viscosity of the concrete mixture. The use of active mineral admixtures also increased the compressive strength and reduced the presence and size of large portlandite crystals in the concrete interface zone. In addition, the active mineral admixtures moderately reduced porosity, which improved the durability of the concrete.
- The use of microsilica and metakaolin in the composition of SDS increased important performance characteristics, such as increasing the frost resistance by 100 cycles, and reduced the volumetric water absorption of concrete by 30–35% and shrinkage deformations by 32%. Apparently, when introducing mineral fillers in mixtures, there is a significant additional interface surface: “additive–water”. Products of cement hydration are deposited on the surface of mineral additive particles, and the smallest particles serve as centers of crystallization and formation of highly stable, low-basicity hydrosilicates and calcium hydroaluminates. The combination of these factors leads to an increase in the degree of hydration, a decrease in the intensity of  $\text{C}_3\text{S}$ , and, accordingly, compaction and hardening of the cement paste.
- As the data of the production tests have shown, microsilica and metakaolin can be recommended for use in production. Here in Kazakhstan, all other conditions being equal, it is more effective to use microsilica in self-compacting concrete for the

production of goods where environmental and economic factors are concerned; the cost of microsilica, which is a waste product of ferrosilicon production, is c. USD 50 per 1 ton, while the cost of metakaolin is about USD 100. Also, by using microsilica, the issue of technogenic waste utilization is resolved, thus achieving a positive impact on the environment and an improvement in the ecology of the region.

- Future work should address alkaline reactivity testing and study of the corrosion resistance of the SCC mortar compositions.

**Author Contributions:** Conceptualization, T.A. and D.A.A.; methodology, T.A.; validation, T.A., D.A.A. and Z.O.Z.; formal analysis, Y.B.U.; investigation, Y.B.U.; resources, M.M.B., D.K.S. and E.I.K.; data curation, M.T.K.; writing—original draft preparation, T.A.; writing—review and editing, D.A.A. and T.A.; visualization, M.T.K.; supervision, T.A.; project administration, M.M.B. All authors have read and agreed to the published version of the manuscript.

**Funding:** This research is funded by the Committee of Science of the Ministry of Science and Higher Education of the Republic of Kazakhstan (Grant No. BR21882292—“Integrated development of sustainable construction industries: innovative technologies, optimization of production, effective use of resources and creation of technological park”).

**Data Availability Statement:** The original contributions presented in this study are included in the article. Further inquiries can be directed to the corresponding author.

**Conflicts of Interest:** The authors declare no conflicts of interest.

## References

1. Gesoglu, M.; Güneyisi, E.; Öz, H.Ö.; Yasemin, M.T.; Taha, I. Durability and Shrinkage Characteristics of Self-Compacting Concretes Containing Recycled Coarse and/or Fine Aggregates. *Adv. Mater. Sci. Eng.* **2015**, *2015*, 278296. [[CrossRef](#)]
2. Kolesnikova, I.V.; Suvorov, A.S.; Bekturganova, N.Y. Analysis of Prospects for the Use of Local Raw Materials for the Production of Self-Sealing Concretes in the Republic of Kazakhstan. *Bull. Kazakh Lead. Acad. Archit. Constr.* **2023**, *90*, 110–124. [[CrossRef](#)]
3. Revilla-Cuesta, V.; Skaf, M.; Ortega-López, V.; Manso, J.M. Multi-Parametric Flowability Classification of Self-Compacting Concrete Containing Sustainable Raw Materials: An Approach to Real Applications. *J. Build. Eng.* **2023**, *63*, 105524. [[CrossRef](#)]
4. Barluenga, G.; Palomar, I.; Puentes, J. Hardened Properties and Microstructure of SCC with Mineral Additions. *Constr. Build. Mater.* **2015**, *94*, 728–736. [[CrossRef](#)]
5. Nurymbetova, R.; Ristavletov, R.; Suzev, N.; Kalshabekova, E.; Kudabayev, R. Concretes Based on Technogenic Wastes Formed during the Mechanical Processing of Carbonate Rocks. *Technobius* **2024**, *4*, 0061. [[CrossRef](#)]
6. Güneyisi, E.; Gesoğlu, M.; Booya, E.; Mermerdaş, K. Strength and Permeability Properties of Self-Compacting Concrete with Cold Bonded Fly Ash Lightweight Aggregate. *Constr. Build. Mater.* **2015**, *74*, 17–24. [[CrossRef](#)]
7. Usanova, K.; Barabanshchikov, Y.; Krasova, A.; Akimov, S.; Belyaeva, S. Plastic Shrinkage of Concrete Modified by Metakaolin. *Mag. Civ. Eng.* **2021**, *103*, 10314. [[CrossRef](#)]
8. Sabitov, Y.; Dyusseminov, D.; Bazarbayev, D. Effect of Modifiers and Mineral Additives from Industrial Waste on the Quality of Aerated Concrete Products. *Technobius* **2021**, *1*, 0010. [[CrossRef](#)]
9. Elyamany, H.E.; Abd Elmoaty, A.E.M.; Mohamed, B. Effect of Filler Types on Physical, Mechanical and Microstructure of Self Compacting Concrete and Flow-Able Concrete. *Alex. Eng. J.* **2014**, *53*, 295–307. [[CrossRef](#)]
10. Strokova, V.V.; Stojkovich, N.; Laketich, S.K.; Zhao, P.; Laketich, A.; Laketich, N. High-Permeable Concrete with Drainage Effect: Analysis of the State and Prospects of Development. *Stroit. Mater.* **2020**, *780*, 32–61. [[CrossRef](#)]
11. Vivek, S.S.; Karthikeyan, B.; Selvaraj, S.K.; Pradeep Kumar, M.; Chadha, U.; Das, S.; Ranjani, G.; Rajasakthivel, R.; Tamilvendhan, K.; Adane, T.M. A Comprehensive Study on Physico-Mechanical Properties of Non-Metallic Fibre Reinforced SCC Blended with Metakaolin and Alcofine. *Mater. Res. Express* **2022**, *9*, 125301. [[CrossRef](#)]
12. Vivek, S.S.; Karthikeyan, B.; Kanna, G.R.; Selvaraj, S.K.; Jose, S.; Palanisamy, P.; Adane, T.M. Study on Fresh and Mechanical Properties of Polyblend Self-Compacting Concrete with Metakaolin, Lightweight Expanded Clay Aggregate, and SAP as Alternative Resources. *Adv. Civ. Eng.* **2022**, *2022*, 2350447. [[CrossRef](#)]
13. Shon, C.-S.; Kim, Y.-S. Evaluation of West Texas Natural Zeolite as an Alternative of ASTM Class F Fly Ash. *Constr. Build. Mater.* **2013**, *47*, 389–396. [[CrossRef](#)]

14. Akhmetov, D.; Akhazhanov, S.; Jetpisbayeva, A.; Pukharenko, Y.; Root, Y.; Uteпов, Y.; Akhmetov, A. Effect of Low-Modulus Polypropylene Fiber on Physical and Mechanical Properties of Self-Compacting Concrete. *Case Stud. Constr. Mater.* **2022**, *16*, e00814. [CrossRef]
15. Su, Y.; Luo, B.; Luo, Z.; Huang, H.; Li, J.; Wang, D. Effect of Accelerators on the Workability, Strength, and Microstructure of Ultra-High-Performance Concrete. *Materials* **2022**, *15*, 159. [CrossRef]
16. Cheah, C.B.; Chow, W.K.; Oo, C.W.; Leow, K.H. The Influence of Type and Combination of Polycarboxylate Ether Superplasticizer on the Mechanical Properties and Microstructure of Slag-Silica Fume Ternary Blended Self-Consolidating Concrete. *J. Build. Eng.* **2020**, *31*, 101412. [CrossRef]
17. ISO/TS 21383:2021; Microbeam Analysis—Scanning Electron Microscopy—Qualification of the Scanning Electron Microscope for Quantitative Measurements. International Organization for Standardization: Geneva, Switzerland, 2021; p. 59.
18. ASTM C1365-18; Standard Test Method for Determination of the Proportion of Phases in Portland Cement and Portland-Cement Clinker Using X-Ray Powder Diffraction Analysis. ASTM International: West Conshohocken, PA, USA, 2018; p. 11.
19. Akimbekova, S.; Aruova, L.; Urkinbayeva, Z.; Nykiel, M. Heat-Resistant Concretes Based on Cement Binders and Waste from the Metallurgical Industry. *Technobius* **2024**, *4*, 0068. [CrossRef]
20. EN 197-1:2011; Cement—Part 1: Composition, Specifications and Conformity Criteria for Common Cements. British Standards Institution: London, UK, 2011; p. 38.
21. GOST 8736-2014; Sand for Construction Works. Specifications. Standardinform: Moscow, Russia, 2014; p. 21.
22. EN 12620:2013; Aggregates for Concrete. British Standards Institution: London, UK, 2013; p. 54.
23. EN 13263-1:2005+A1:2009; Silica Fume for Concrete—Part 1: Definitions, Requirements and Conformity Criteria. British Standards Institution: London, UK, 2009; p. 23.
24. GOST 30459-2008; Admixtures for Concretes and Mortars. Determination and Estimate of the Efficiency. Standardinform: Moscow, Russia, 2008; p. 18.
25. Okamura, H.; Ouchi, M. Self-Compacting Concrete. *J. Adv. Concr. Technol.* **2003**, *1*, 5–15. [CrossRef]
26. Self-Compacting Concrete European Project Group. *The European Guidelines for Self-Compacting Concrete: Specification, Production and Use*; International Bureau for Precast Concrete (BIBM): Brussels, Belgium, 2005; p. 68.
27. Balabanov, M.S.; Daxno, I.A. Methods for Selecting Composition of Self-Compact Concretes. In Proceedings of the Traditions and Innovations in Construction and Architecture, Building Technologies, Samara, Russia, 26–30 October 2020; pp. 39–48.
28. EN 196-6:2018; Methods of Testing Cement—Part 6: Determination of Fineness. British Standards Institution: London, UK, 2018; p. 18.
29. EN 196-3:2016; Methods of Testing Cement—Part 3: Determination of Setting Times and Soundness. British Standards Institution: London, UK, 2016; p. 26.
30. EN 12350-8:2019; Testing Fresh Concrete—Part 8: Self-Compacting Concrete—Slump-Flow Test. British Standards Institution: London, UK, 2019; p. 8.
31. EN 12350-8:2019; Testing Fresh Concrete—Part 9: Self-Compacting Concrete—V-Funnel Test. British Standards Institution: London, UK, 2019; p. 6.
32. EN 206:2013+A1:2016; Concrete—Specification, Performance, Production and Conformity. British Standards Institution: London, UK, 2016; p. 92.
33. GOST 10060-2012; Concretes. Methods for Determination of Frost-Resistance. Standardinform: Moscow, Russia, 2012; p. 24.
34. GOST 12730.3-2020; Concretes. Method of Determination of Water Absorption. Standardinform: Moscow, Russia, 2020; p. 14.
35. GOST 24544-2020; Concretes. Methods of Shrinkage and Creep Flow Determination. Standardinform: Moscow, Russia, 2020; p. 30.
36. EN 196-2:2013; Method of Testing Cement—Part 2: Chemical Analysis of Cement. British Standards Institution: London, UK, 2013; p. 73.
37. GOST 8267-93; Crushed Stone and Gravel of Solid Rocks for Construction Works. Specifications. Standardinform: Moscow, Russia, 2018; p. 14.
38. Enterprise Standard 46976-1901-21-002-2014; Condensed Microsilica. Tau-Ken Temir, LLP: Karaganda, Kazakhstan, 2014; p. 1.
39. Smirnov, P.V.; Zhakipbayev, B.E.; Staroselets, D.A.; Deryagina, O.I.; Batalin, G.A.; Gareev, B.I.; Vergunov, A.V. Diatomites and Opoka from Western Kazakhstan Deposits: Lithogeochemistry, Structural and Textural Parameters, Potential of Use. *Bull. Tomsk Polytech. Univ. Geo Assets Eng.* **2023**, *334*, 187–201. [CrossRef]
40. Plast-Rifey Metakaolin MKZL. Available online: <http://eng.kaolinzh.ru/production-from-kaolin-clay/metakaolin-mkzl/> (accessed on 13 April 2025).
41. Zakharov, S.A. The Advantages of High Reactivity Metakaolin Application in Concrete and Dry Construction Mixtures. *ALITin-form Cem. Beton Suhie Smesi* **2008**, *2*, 52–57.
42. Akhmetov, D.; Aniskin, A.; Uteпов, Y.; Root, Y.; Kozina, G. Determination of Optimal Fibre Reinforcement Parameters for Self-Compacting Concretes. *Teh. Vjesn.-Tech. Gaz.* **2020**, *27*, 1982–1989. [CrossRef]
43. Uteпов, Y.; Akhmetov, D.; Akhmatshaeva, I. Effect of Fine Fillers from Industrial Waste and Various Chemical Additives on the Placeability of Self-Compacting Concrete. *Comput. Concr.* **2020**, *25*, 59–65. [CrossRef]

44. Abdraimov, I.; Kopzhassarov, B.; Kolesnikova, I.; Akhmetov, D.A.; Madiyarova, I.; Utepov, Y. Frost-Resistant Rapid Hardening Concretes. *Materials* **2023**, *16*, 3191. [[CrossRef](#)]
45. Zhakipbekov, S.; Aruova, L.; Toleubayeva, S.; Ahmetganov, T.; Utkelbaeva, A. The Features of the Hydration and Structure Formation Process of Modified Low-Clinker Binders. *Mag. Civ. Eng.* **2021**, *103*, 10302. [[CrossRef](#)]
46. Yu, R.; Spiesz, P.; Brouwers, H.J.H. Effect of Nano-Silica on the Hydration and Microstructure Development of Ultra-High Performance Concrete (UHPC) with a Low Binder Amount. *Constr. Build. Mater.* **2014**, *65*, 140–150. [[CrossRef](#)]
47. Shannag, M.J. High Strength Concrete Containing Natural Pozzolan and Silica Fume. *Cem. Concr. Compos.* **2000**, *22*, 399–406. [[CrossRef](#)]
48. Wild, S.; Khatib, J.M.; Jones, A. Relative Strength, Pozzolanic Activity and Cement Hydration in Superplasticised Metakaolin Concrete. *Cem. Concr. Res.* **1996**, *26*, 1537–1544. [[CrossRef](#)]
49. Siddique, R. Properties of Self-Compacting Concrete Containing Class F Fly Ash. *Mater. Des.* **2011**, *32*, 1501–1507. [[CrossRef](#)]
50. Zhanikulov, N.N.; Khudyakova, T.M.; Taimassov, B.T.; Sarsenbayev, B.K.; Dauletiarov, M.S.; Kolesnikov, A.S.; Karshygayev, R.O. Receiving Portland Cement from Technogenic Raw Materials of South Kazakhstan. *Eurasian Chem.-Technol. J.* **2019**, *21*, 333. [[CrossRef](#)]
51. Singh, E.R.; Saini, E.L.; Sharma, E.T. Curing of Concrete: A Technical Study to Increase Rate of Curing. *Int. J. Adv. Eng. Technol.* **2014**, *49*, 53.
52. Nunes, S.; Oliveira, P.M.; Coutinho, J.S.; Figueiras, J. Rheological Characterization of SCC Mortars and Pastes with Changes Induced by Cement Delivery. *Cem. Concr. Compos.* **2011**, *33*, 103–115. [[CrossRef](#)]
53. Zhagifarov, A.; Talal, A.; Akhmetov, D.; Suzev, N.; Kolesnikova, I. Effectiveness of Road Slabs Produced Using Microsilica and Fiber Quality Improvement. *Int. J. GEOMATE* **2025**, *28*, 16–24. [[CrossRef](#)]

**Disclaimer/Publisher’s Note:** The statements, opinions and data contained in all publications are solely those of the individual author(s) and contributor(s) and not of MDPI and/or the editor(s). MDPI and/or the editor(s) disclaim responsibility for any injury to people or property resulting from any ideas, methods, instructions or products referred to in the content.